Alterations in Alveolar Basement Membranes During Postnatal Lung Growth

JEROME S. BRODY, CHARLES A. VACCARO, PEGGY JO GILL, and JEREMIAH E. SILBERT
Pulmonary Medicine Section, Boston City and University Hospitals, Boston University School of Medicine; and the Veterans Administration Outpatient Clinic and Department of Medicine, Harvard Medical School, Boston, Massachusetts 02118

ABSTRACT We studied the ultrastructural characteristics of alveolar basement membranes (ABM) and capillary basement membranes (CBM) in rat lungs at birth, at 8–10 d of age, during alveolar formation, and at 6–10 wk of age, after most alveoli have formed. We also measured in vitro lung proteoglycan and heparan sulfate synthesis at each age. We noted three major age-related changes in pulmonary basement membranes. (*a*) Discontinuities in the ABM through which basilar cytoplasmic foot processes extend are present beneath alveolar type-2 cells but not alveolar type-1 cells. These discontinuities are most prevalent at birth but also exist in the adult. (*b*) Discontinuities are also present in CBM at the two earliest time points but are maximal at 8 d of age rather than at birth. Fusions between ABM and CBM are often absent at 8 d of age, but CBM and CBM/ABM fusions were complete in the adult. (*c*) Heparan sulfate proteoglycans identified with ruthenium red and selective enzyme degradation are distributed equally on epithelial and interstitial sides of the ABM lamina densa at birth, but decrease on the interstitial side with age. In vitro proteoglycan and heparan sulfate accumulation at birth was two times that at 8 d and five times that in the adult. Discontinuities in ABM allow epithelial-mesenchymal interactions that may influence type-2 cells cytodifferentiation. Discontinuities in CBM suggest that capillary proliferation and neovascularization are associated with alveolar formation at 8 d. When CBM becomes complete and forms junctions with ABM, lung neovascularization likely ends as does the ability to form new alveoli.

The lung parenchyma of most mammalian species contains few recognizable gas exchange units (alveoli) at birth (1). The majority of alveoli develop postnatally in a short period of time ranging from days in small rodents to years in man (1, 2). After this intense period of restructuring of the gas exchange surface of the lung, few new alveoli form under normal circumstances. Furthermore, once this period of postnatal morphogenesis has passed, the mature lung appears incapable of forming large numbers of new alveoli in response to growth stimuli such as pneumonectomy (3). Thus the circumstances associated with formation of lung gas exchange units appear to be unique and limited to a relatively short period of postnatal life.

Basement membranes have been shown to play an important role in regulating tissue morphogenesis in a number of organs (4). Much of this role involves regulation of the interface between epithelium and mesenchyme and regulation of proliferation and differentiation of key cells in the morphogenic process. Basement membranes also compartmentalize tissues, thus contributing to their structural organization. These basement membrane developmental functions have been demonstrated in tissues as diverse as cornea (5), tooth (6), and kidney (7, 8), and in branching organs such as salivary and mammary gland (9–11). Branching morphogenesis of the bronchial tree in fetal life also seems to involve interaction of epithelium and mesenchyme, most likely regulated by airway basement membranes (12–15). However, little information exists relating to the role that basement membranes might play in development of the gas exchange surfaces of the lung during postnatal life.

Because the process of postnatal alveolar formation involves tissue compartmentalization, cell proliferation and differentiation, and most probably epithelial-mesenchymal interactions, it seems likely that components of basement membranes would be important determinants of postnatal alveolarization. We have therefore applied methods for highlighting basement membrane components previously used by us for defining the ultrastructure of alveolar wall basement membranes in the adult rat (16, 17) to define changes that occur in basement membranes during postnatal formation of alveoli. We have

THE JOURNAL OF CELL BIOLOGY · VOLUME 95 NOVEMBER 1982 394-402

studied the rat lung, because the stereology (2), morphology (18), and physiology (19) of lung growth in this animal is so well defined. We show that there is considerable restructuring of both alveolar (ABM) and capillary (CBM) basement membranes during the early postnatal period; that epithelial-mesenchymal interactions may be involved in early postnatal lung growth; and that neovascularization and compartmentalization of the alveolar wall by capillary basement membranes is an important facet of lung structuring at this stage and may be linked to the inability of adult lung to form new alveoli. We also demonstrate an age-related change in the distribution but not type of alveolar basement membrane-associated proteoglycans and show that synthesis of sulfated proteoglycans is greater in newborn than in adult lung.

MATERIALS AND METHODS

We studied rats between birth and 6–10 wk of age. Animals were raised from litters that were adjusted to eight pups per mother at birth. Four to six animals per age group were sacrificed by intraperitoneal injection of 2 mg/100 g body weight of sodium pentobarbitol.

Tannic Acid Fixation

In most animals the trachea was exposed and cannulated and the lungs were inflated to 25–30 cm H_2O pressure with 1% tannic acid and 2% glutaraldehyde in 0.075 M phosphate buffer pH 7.2–7.3. The chest cavity was opened and random samples of each lobe were excised, minced into 1–2-mm cubes, and placed in fresh fixative for 2–3 h at room temperature. Following tannic acid/glutaraldehyde fixation, tissue blocks were rinsed four times over 10 min with 0.075 M phosphate buffer containing 0.18 M sucrose. Tissue blocks were postfixed for 1–2 h in 1% osmium tetroxide in phosphate buffer with sucrose at room temperature. After osmium fixation, the tissue was quickly rinsed in two changes of buffer and rapid-processed through ascending concentrations of acetone. Blocks were infiltrated in a mixture of Poly 812, Araldite 502, DDSA, and DMP-30 split 50:50 with acetone for 20 min on a standard rotor. Final infiltration included two additional changes of 100% resin mixture for 30 min on the rotor. Blocks were embedded in fresh resin and polymerized at 60°C for 1 h. Before thin sectioning, the plastic was further polymerized for 1 h at 100°C. Routine thin sections were obtained with glass or diamond knives and stained with uranyl acetate and lead citrate. Electron micrographs were prepared with a Philips EM 300 electron microscope.

Ruthenium Red Staining

Additional animals from each age group were sacrificed and lungs were inflated with a 1% Triton X-100 and 1% ruthenium red mixture in McIlvaine's buffer pH 5.6. Samples of the whole lung were excised and incubated in fresh buffered detergent with ruthenium red for 1 h with gentle agitation. The detergent Triton was used to maximize penetration and staining by ruthenium red of basement membrane anionic sites (16). Tissue samples were fixed in 5% glutaraldehyde plus 1% ruthenium red in McIlvaine's buffer overnight at 4°C. The next day, the blocks were washed four times, 5 min each with fresh buffer containing ruthenium red, and postfixed for 1–2 h in 1% osmium tetroxide in McIlvaine's containing 0.75% ruthenium red. Tissue samples were rapid-processed through acetone and embedded in plastic using the method in Section A.

Characterization of Basement Membrane Anionic Sites

Minced pieces of perfused lung were washed with sterile Minimum Essential Medium (MEM). 40–50 pieces were placed in a 25 cm^2 flask in 8 ml of MEM containing 10% fetal calf serum and 2 mM glutamine. The MEM was sulfate-free, having $MgCl_2$ substituted for $MgSO_4$. 800 μCi of $Na_2{}^{35}SO_4$ (200 μCi/mm) was added to the 8 ml of complete medium and incubated for 20 h at 37°C in 5% CO_2 and air in order to provide uniform labeling of newly synthesized [^{35}S]-proteoglycans.

The tissue pieces were removed and washed repeatedly with iced PBS containing 0.68 mM $CaCl_2$ and 0.4 mM $MgSO_4$. When the tissue pieces were free of $Na_2{}^{35}SO_4$, they were incubated with additional phosphate-buffered saline (PBS), chondroitinase ABC, or crude *Flavobacter heparinum* enzyme.

Chondroitinase ABC (Miles Laboratories Inc., Elkhart, IN) was used at a concentration of 0.5 U/1.0 ml of PBS added to tissue pieces. This enzyme is known to selectively degrade dermatan sulfate, chondroitin 4-sulfate, and chondroitin 6-sulfate (20). *F. heparinum* enzyme was prepared as previously described (21) by sonication of lyophilized bacteria followed by filtration to remove particulate matter, and was used at a concentration of 3 U/1.0 ml of PBS added to tissue pieces (21). This enzyme preparation contains chondroitinase, dermatanase, heparinase, and heparanase activity and thus will degrade all sulfated glycosaminoglycans except keratan sulfate (22). It has been previously shown that the preparation has no detectable collagenase, protease, sialidase, or fucosidase activities (21) and thus would appear to be specific for glycosaminoglycans. Control and enzyme-treated lung pieces were incubated at 37°C for 30 min.

Following enzyme digestion, the tissues were removed, washed, and analyzed for the remaining proteoglycans. (*a*) Pieces were incubated at 37°C in 0.5 M NaOH overnight. Following extraction, the solubilized glycosaminoglycans were freed of [^{35}S]sulfate by separation on a Sephadex G-25 column. The isolated [^{35}S]glycosaminoglycans were incubated with PBS, chondroitinase ABC, or *F. heparinum* enzyme at 37°C for 40 min and applied to a Sephadex G-50 column to separate the remaining glycosaminoglycans from degradation products. (*b*) Tissue samples taken before and after enzyme digestion were fixed with glutaraldehyde containing ruthenium red stain, prepared for electron microscopy, and utilized for morphometry of basal membrane anionic sites.

Morphometry of Basement Membrane Anionic Sites and Type 2 Cell Basilar Processes

Tissue samples of three animals from each age group stained with ruthenium red and subsequently prepared for electron microscopy were utilized for morphometry of basement membrane anionic sites. 30 pictures per animal were taken at random of the alveolar and capillary basement membranes. All negatives were enlarged to the same print magnification to count ruthenium red-positive sites. Areas of basement membrane that were tangentially sectioned or did not contain a lamina densa were discarded. We measured the length and counted the total number of ruthenium red granules associated with ABM and CBM present in each micrograph. The total numbers of sites on either side and in the center of the lamina densa associated with the ABM were separately counted and recorded.

Tissue samples from lungs to two - three animals from each age group, fixed with tannic acid as described above, were utilized for analysis of alveolar type-2 cell foot processes, and ABM and CBM morphometry. 30 type-2 cells per animal were randomly observed and recorded. For each type-2 cell, we counted the number of basilar cytoplasmic processes and the number of times these processes penetrated the lamina densa. We also followed the lamina densa around the basal cell membrane associated with each type-2 cell and rated its continuity between 0 and 100%. 30 capillaries were also randomly observed per animal per each group fixed in tannic acid. The amount of CBM covering each capillary unit was rated between 0 and 100% and separately recorded.

RESULTS

The change in lung structure that occurs over the first 21 d of postnatal life is illustrated in Fig. 1. At birth, lung parenchyma consists of thick-walled, cellular saccules with capillaries facing airspace on each side of the saccule. By 8 d of life, saccule walls have thinned and become less cellular and buds of new alveoli have begun to form. By 21 d, alveoli are thin, relatively acellular, and contain a single rather than double capillary network.

Fig. 2 illustrates alveolar basement membrane (ABM) beneath an alveolar type-2 cell at birth. There are large areas of the cell under which no ABM appears. In addition, several cytoplasmic foot processes extend from the basilar surface of the type-2 cell into the interstitium. Average ABM continuity was 76 ± 2% (SEM) beneath type-2 cells at birth, 86 ± 2% at 8 d, and 90 ± 2% in the adult (see Fig. 3). Although the number of basilar foot processes was similar at all ages, twice as many of these foot processes extended into the interstitium at birth compared with the other ages. The ABM was continuous beneath alveolar type-1 cells at all ages and in no instance did ABM penetrating foot processes appear beneath type-1 cells. In the adult alveolar wall, capillaries are virtually completely encircled by basement membrane: ABM on the thin side of the alveolus and CBM on the thick or interstitial side (Fig. 4*a*). Fig. 5 shows that CBM covered 99 ± 2% of capillary interstitial

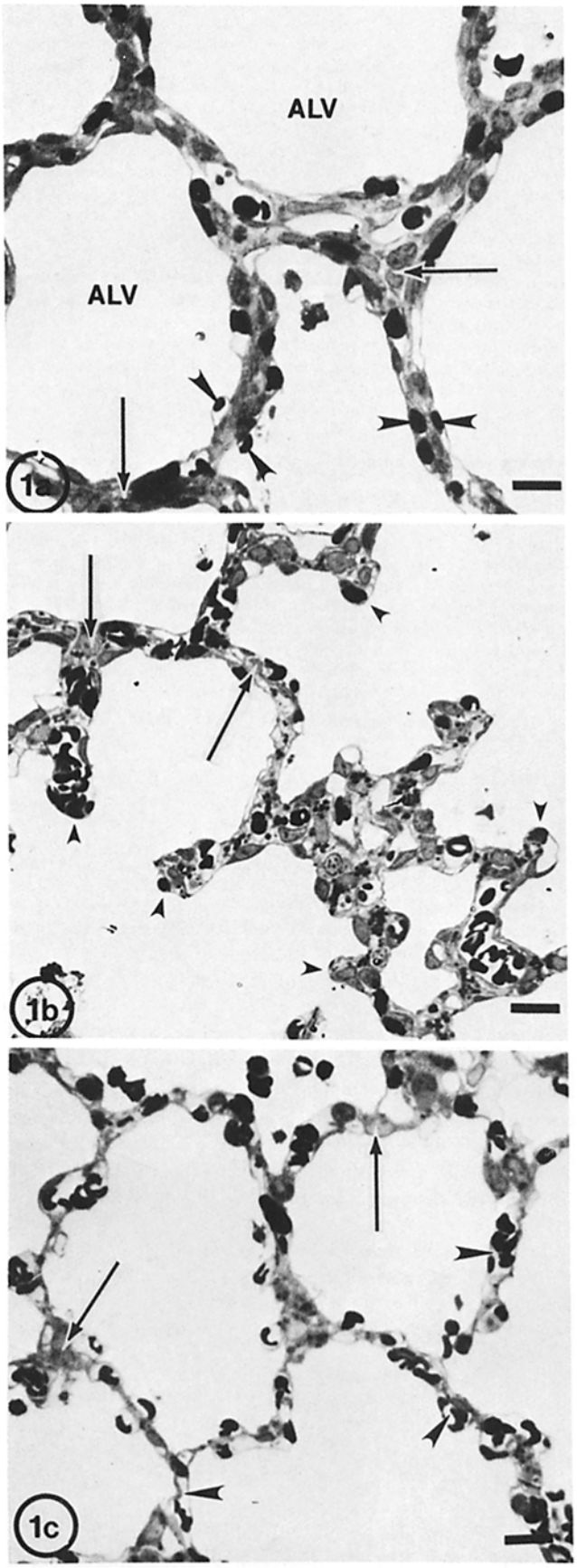

FIGURE 1 Inflated lungs from newborn, 8-d-old and 10-wk-old rats. All (*a*) Newborn rat: large air saccules (*ALV*) contain an extensive capillary network (arrowheads point to intraluminal red blood cells) in which double set of capillaries are separated by a thick cellular interstitium (arrows). (*b*) Eight-day-old rat: the interstitium (arrows) is more cellular and new alveolar septal buds (arrow heads) are in various stages of development. (*c*) 10-wk-old rat: alveolar walls have thinned, capillaries (arrow heads) are not now separated into a dual network by the interstitium (arrows) which is less cellular. *a*, *b*, and *c*: bars, 1 μm. × 520.

side surface in the adult and that no capillaries had CBM discontinuities of >10% of their surface. In contrast, capillaries at birth often had large areas without CBM (see Fig. 4*b*). Approximately one-third of capillaries were completely covered by CBM, one-third were 90–99% covered, and one-third were 70–90% covered, i.e., 10–30% of their surface had no CBM (see Fig. 5). Junctions between CBM and ABM that serve to fix the capillary in place, forming the thin side of the alveolar wall in the adult, were often absent in this group of capillaries (see Fig. 4*c* and *d*). At 8 d, average CBM continuity fell to 72%, and >40% of capillaries appeared to have <70% CBM covering (see Fig. 5). The number of capillaries completely covered by CBM fell to <20%. Junctions between CBM and ABM were often absent in capillaries with large CBM discontinuities. In addition, capillaries at birth and at 8 d were often lined by endothelial cells that had sproutlike projections that on occasion formed small luminal and abluminal channels (see Fig. 6). In contrast, capillaries in the adult were covered by smooth nonconvoluted endothelial cells.

Fig. 7 illustrates a third age-related feature of ABM. At birth, ruthenium red-staining anionic sites appear on both the epithelial (luminal) and interstitial or endothelial (abluminal) sides of ABM. There are fewer abluminal anionic sites at 8 d and even fewer in the adult. These differences are accentuated in ABM sectioned in a tangential plane (Fig. 7*d* and *e*). Fig. 8 shows that the relative distribution of luminal to abluminal sites is 1.4:1 at birth and changes to 4.6:1 or almost five luminal for every abluminal site in the adult. The change in distribution is due primarily to a decrease in abluminal sites from 1.01 to 0.38 sites/nm rather than an increase in the number of luminal sites, which remains relatively constant (see Table I). We have previously shown that in the adult all ruthenium red-positive anionic sites on the ABM represent heparan sulfate proteoglycans. Selective enzyme degradation studies demonstrate that all ABM anionic sites are heparan sulfate at birth and at 8 d (see Fig. 9).

The net amount of [^{35}S]proteoglycan formed in the perfused minces is shown in Table II. Newborn lung accumulated more than twice as much [^{35}S]sulfate as 8-d lung and 15 times as much as adult lung. However, the newborn lung was slightly more cellular (based on DNA/mg protein) than 8-d lung and almost three times more cellular than adult lung. Thus when the [^{35}S]proteoglycan was analyzed on a per cell basis, the newborn lung was seen to accumulate approximately twice as much [^{35}S]proteoglycan as the 8-d lung, and approximately five times as much as the adult lung. When aliquots of [^{35}S]glycosaminoglycan were incubated with chondroitinase ABC, ~70–75% was degraded (Fig. 10 and Table II), indicating that [^{35}S]heparan sulfate comprised 25–30% of the [^{35}S]glycosaminoglycan. There were no differences in this proportion between newborn, 8-d, or adult. Incubation with crude *F. heparinum* enzyme resulted in degradation of all the [^{35}S]glycosaminoglycans. Thus, both heparan sulfate accumulation and chondroitin sulfate accumulation decreased equally from newborn to adult.

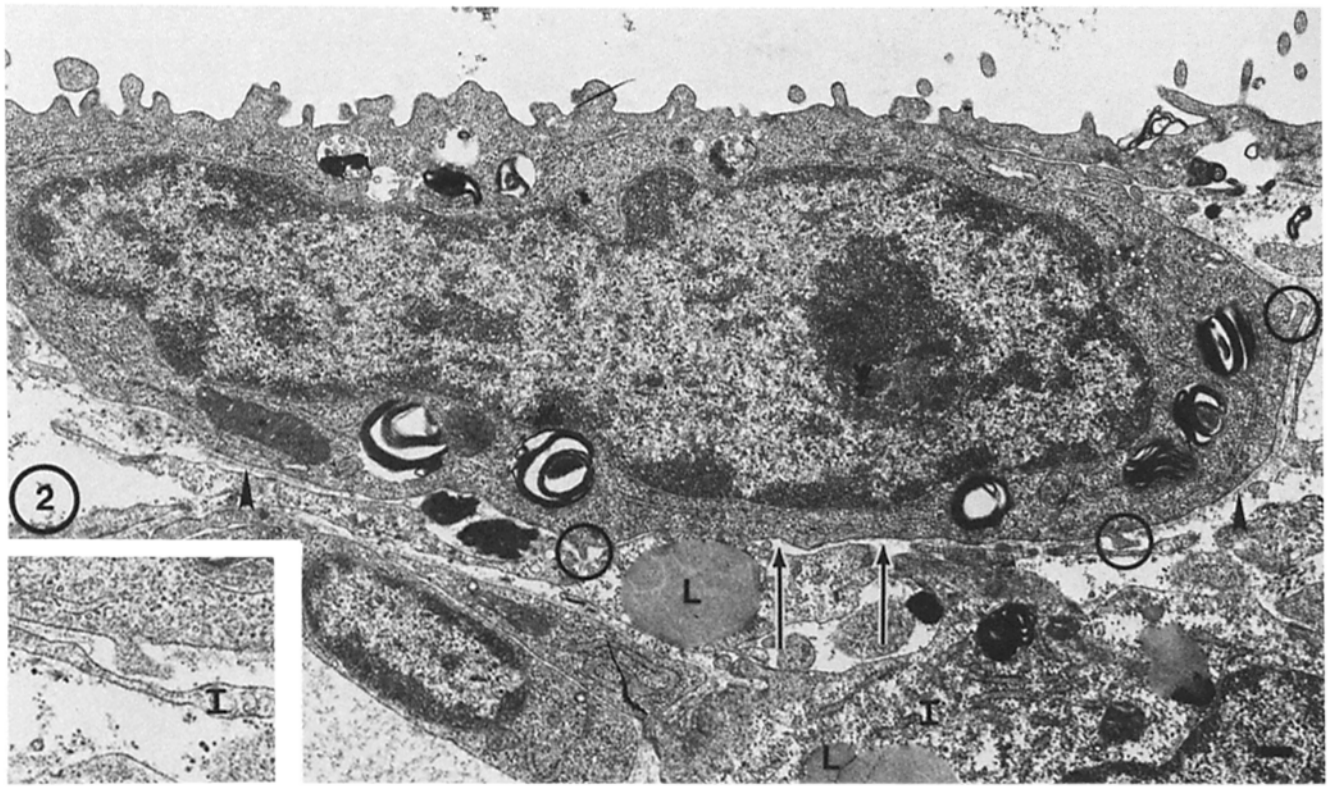

FIGURE 2 The alveolar basement membrane (arrowheads) beneath type-2 cells at birth is often patchy and incomplete (arrows). Basilar cytoplasmic foot processes (circled) often penetrate through gaps in the ABM and appear in close approximation to interstitial cells (*I*), some of which contain neutral lipid droplets (*L*). Bar, 0.1 μm. × 15,333. *Inset*: a penetrating foot process adjacent to a fragment of an interstitial cell. × 33,174.

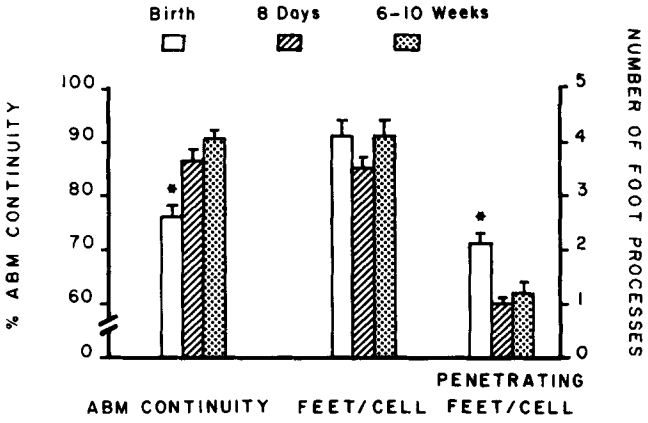

FIGURE 3 Counts of ABM continuity, number of type-2 cell basilar foot processes per cell, and number of those feet that penetrate the ABM per cell. Mean values ± 1 SEM. Asterix over bars at birth indicate that these values differ ($p < .01$) from those at two other ages.

DISCUSSION

We have described three major changes that occur in the ultrastructure of alveolar wall basement membranes during early postnatal lung growth. First, large discontinuities appear in the ABM beneath alveolar type-2 cells at birth. Alveolar basement membranes beneath type-2 cells become more complete at 8 d of age and in the adult although basilar cytoplasmic foot processes from these cells extend into the interstitium at all ages. Second, discontinuities appear in the CBM at birth and increase in degree at 8 d of age during the time of peak alveolar proliferation. The CBM becomes complete as do fusions between CBM and ABM in the adult. Third, heparan sulfate proteoglycans are evenly distributed on luminal and abluminal sides of the ABM at birth; however, there is a progressive decrease in the percent and linear density of abluminal proteoglycans at 8 d of age and in the adult. These observations have been coupled with data showing that in vitro lung proteoglycan accumulation at birth is twice that at 8 d of age and five times that of the adult. Despite the dramatic decrease in lung proteoglycan accumulation that occurs with age, heparan sulfate accounts for 25–30% of proteoglycan synthesis at each age. We believe that the above observations provide insights into how alveolar walls are structured and how the lung gas exchange surface forms during early postnatal life.

ABM Discontinuities

The discontinuities we have described in ABM are associated with extension of type-2 cell foot processes into the interstitium of the alveolar wall. The link between greater discontinuities and more foot processes extending into the interstitium at birth might be expected from the studies of Sugrue and Hay (23), who showed similar cytoplasmic extensions in corneal epithelial cells in the absence of basement membrane components beneath the cell. The type-2 cell foot processes provide a mechanism for epithelial-mesenchymal interactions within the alveolar wall. There is extensive experience with a number of organs showing that these communications generally involve potential epithelial-mesenchymal contact and can influence the function of both epithelial and mesenchymal cells (5, 24–28).

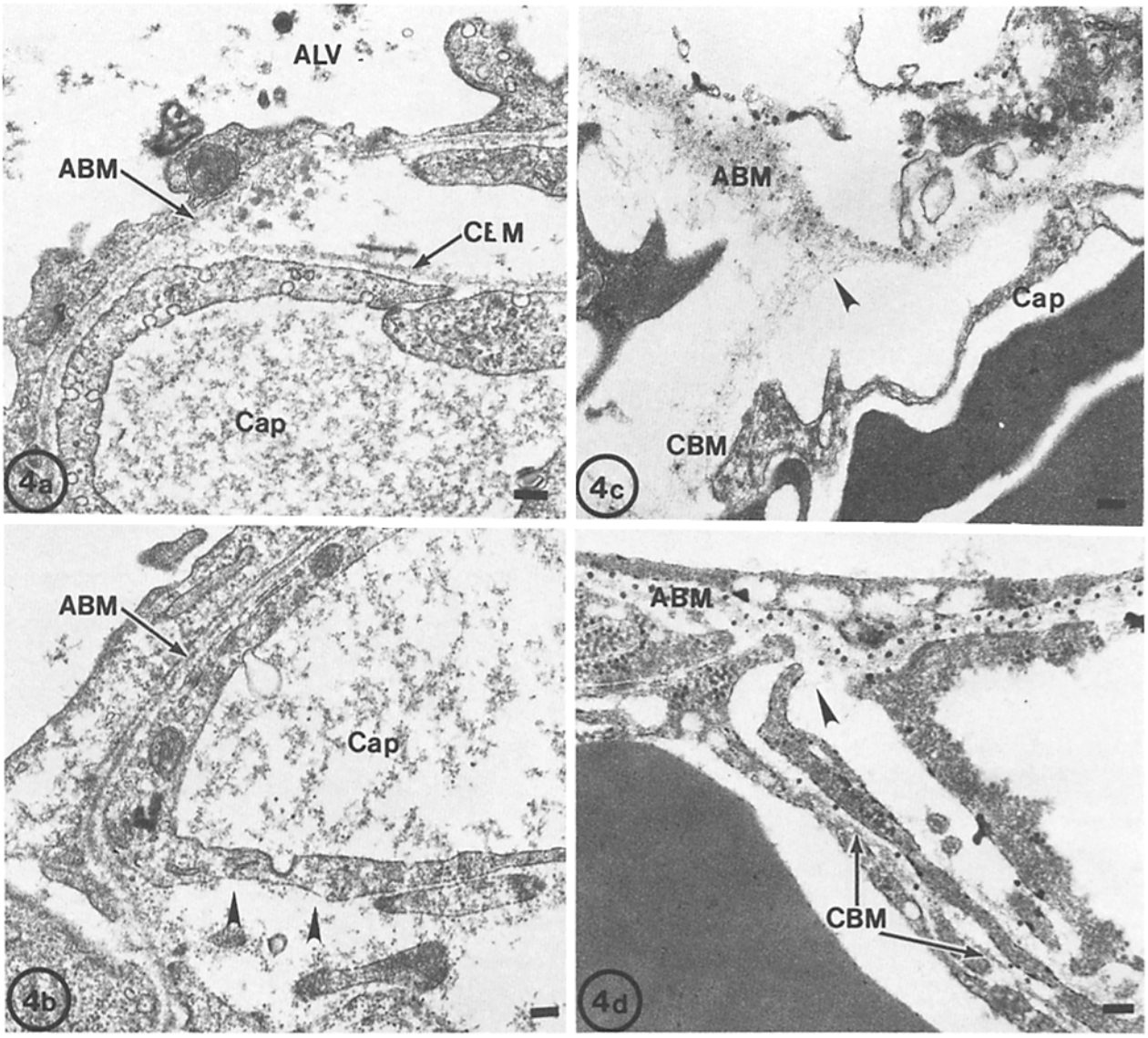

FIGURE 4 (*a*) Tannic acid fixation of adult lung shows alveolus (*ALV*) and capillary (*Cap*), which is covered by *CBM* facing the interstitium (thick side) and by *ABM* where endothelium faces epithelium (thin side). Bar, 0.1 μm. × 45,000. (*b*) Tannic acid fixation of newborn lung shows that capillaries (*Cap*) at birth often have large areas (arrowheads) without *CBM* on the thick side although *ABM* on the thin side is intact. Bar, 0.1 μm. × 39,250. (*c*) Ruthenium red stain of adult lung shows junction between *CBM* and *ABM* (arrowhead) which fixes the capillary (*Cap*) in place against the alveolar epithelium. Bar, 0.1 μm. × 40,370. (*d*) Ruthenium red stain of newborn lung illustrating incomplete *CBM* and absent *ABM-CBM* junction (arrowhead). Bar, 0.1 μm. × 44,688.

Such interactions have been shown to be important in regulating development of the tracheobronchial tree in early fetal life (12–15). There is little information about the involvement of these cell-cell interactions in the development of the pulmonary gas exchange surfaces in late fetal and early postnatal life, although Smith and co-workers (29) have shown that fetal lung fibroblasts produce a factor that stimulates incorporation of precursors into phospholipid in cultures type-2 cells and have suggested that interstitial fibroblasts may produce somatomedin-C, which is a type-2 cell mitogen (30).

The alveolar type-2 cell is a cuboidal, metabolically active cell that synthesizes and secretes a surface tension-lowering phospholipid onto the alveolar surface and that also serves as a stem cell from which the alveolar type-1 cells are derived (31). In a variety of circumstances that includes the late fetal period (32), postnatal lung growth (33), postpneumonectomy compensatory lung growth (34), and lung repair following injury (35, 36), some proliferating type-2 cells are induced by as yet unknown signals to lose their surfactant-synthesizing function and differentiate into type-1 lining cells. The type-1 cell is a long, thin cell with few cytoplasmic organelles that covers >95% of the alveolar surface in the adult rat lung (37).

In late fetal and early postnatal life, the type-2 cell is called upon to perform two distinct functions. The first requires surfactant production in preparation for the transition from liquid to air breathing and involves maturation of the cell's phospholipid synthetic machinery (38). The second function requires formation of additional alveolar surface as the fetal lung first distends with liquid and then expands dramatically during the change to air breathing (39). The timing of appearance of type-2 cell ABM discontinuities in the fetal rat lung has been reported from this laboratory by Grant and co-workers (40). They found that ABM discontinuities begin to appear on fetal days 19 and 20 and are maximal in extent after

birth. There was no correlation between the degree of maturity of the type-2 cell, as judged by number of lamellar bodies, and ABM discontinuity. Thus the timing of ABM discontinuities appears to be most closely related to the perinatal demand for new surface area and differentiation into type-1 alveolar lining cells. Our finding that proteoglycan synthesis, especially heparan sulfate synthesis, is greater at birth, when little interstitial collagen is present (19), than at the other ages studied, suggests that large amounts of new basement membrane are being made at this time. If epithelial-mesenchymal interactions through ABM are important in this process, they may function to stimulate stromal synthesis by the type-2 cell, which is capable of basement membranes in vitro (41). Type-1 cells have no apparent epithelial-mesenchymal contacts and, since these cells derive from type-2 cells, the type-2 cell may produce its own ABM in vivo in the process of lengthening and differentiating into type-1 cells.

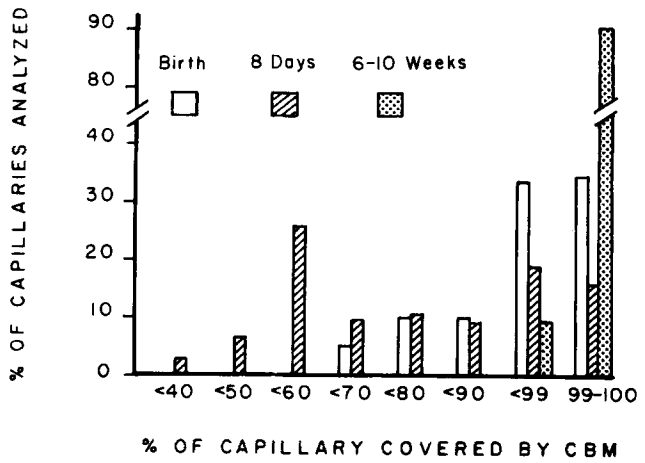

FIGURE 5 Frequency distribution of *CBM* continuity in capillaries at birth, *8 days*, and in adult rat. In the adult, the average capillary is virtually completely covered by *CBM* (99 ± 2 SEM) with >90% of capillaries being completely enclosed by *CBM* (stippled bar). In the newborn, the average capillary *CBM* in 90 ± 12% with ~30% of capillaries having <90% *CBM* (open bars). At *8 d*, when alveolar proliferation is at its peak, average capillary *CBM* is 72 ± 21%. Only 15% of capillaries at this age are completely enclosed by *CBM*, and a large number of capillaries have <60% CBM covering (cross-hatched bars).

CBM Discontinuities

A second major change in alveolar wall basement membranes relates to formation of CBM rather than ABM. At birth, about one-third of capillaries have incomplete or discontinuous CBM. At 8 d of age, when lung alveolarization is at its peak, the vast majority of capillaries have incomplete CBM. In the adult, when alveolarization has slowed or ended virtually all capillaries are completely encompassed by CBM. Furthermore, many capillaries at 8 d are lined by endothelial cells that have fingerlike cytoplasmic protrusions that often form multiple luminal and abluminal channels, whereas adult endothelial cells displayed smooth surfaces without endothelial cytoplasmic projections. These findings are similar to those described in neovascularized tissues (42, 43), suggesting that angiogenesis is an important facet of early postnatal lung growth associated with formation of new alveoli and that local or systemic factors controlling angiogenesis may play an important role in regulating postnatal lung growth.

We have also noted that fusions of CBM with ABM, which serve to lock the capillary in place against the alveolus and isolate capillary endothelium in a sheathlike fashion in the adult (17), are scattered and infrequent at birth and 8 d. This suggests that, when early postnatal CBM formation and fusion to ABM is complete, the neovascularization of the alveolar wall, which characterizes early postnatal lung growth, ends.

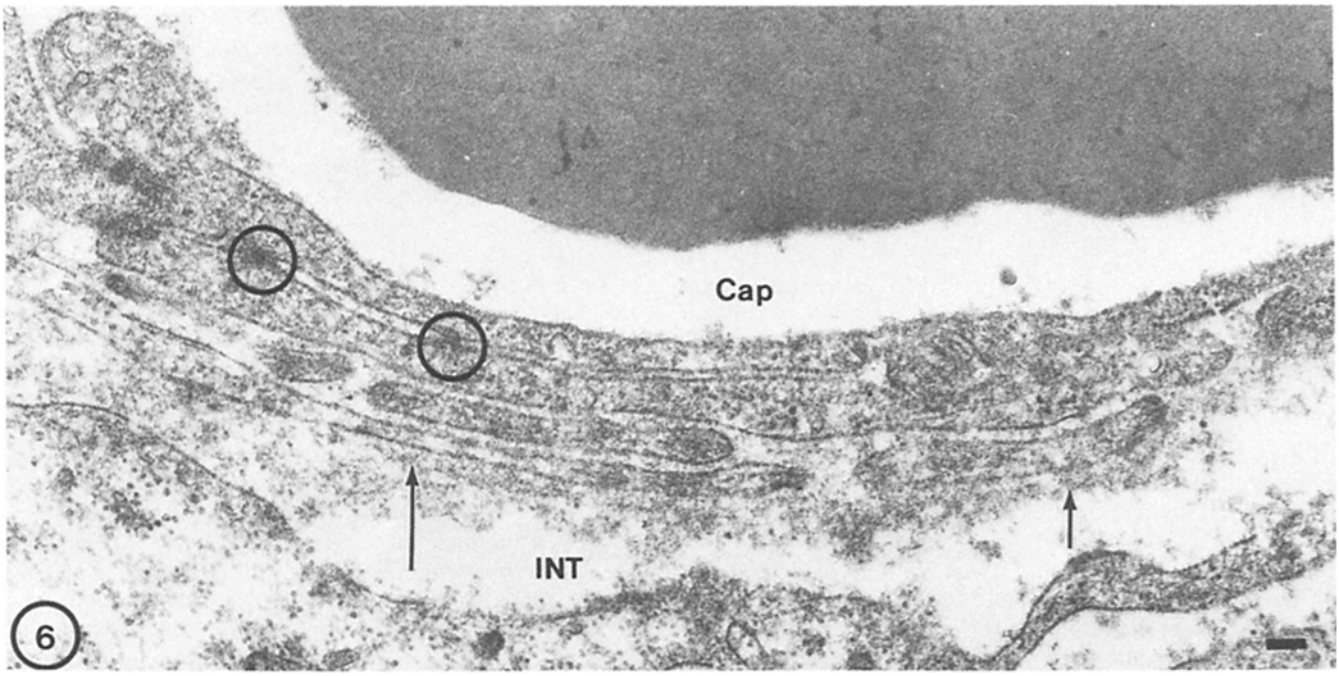

FIGURE 6 Capillary (*Cap*) from 8-d-old rat lung, tannic acid fixation. The endothelium with junctions (circles) contains multiple cell extensions, some facing the luminal surface, others forming layers facing the interstitium (*INT*). CBM (arrows), which is incomplete, appears to surround all endothelial cell layers. Bar, 0.1 μm. × 45,780.

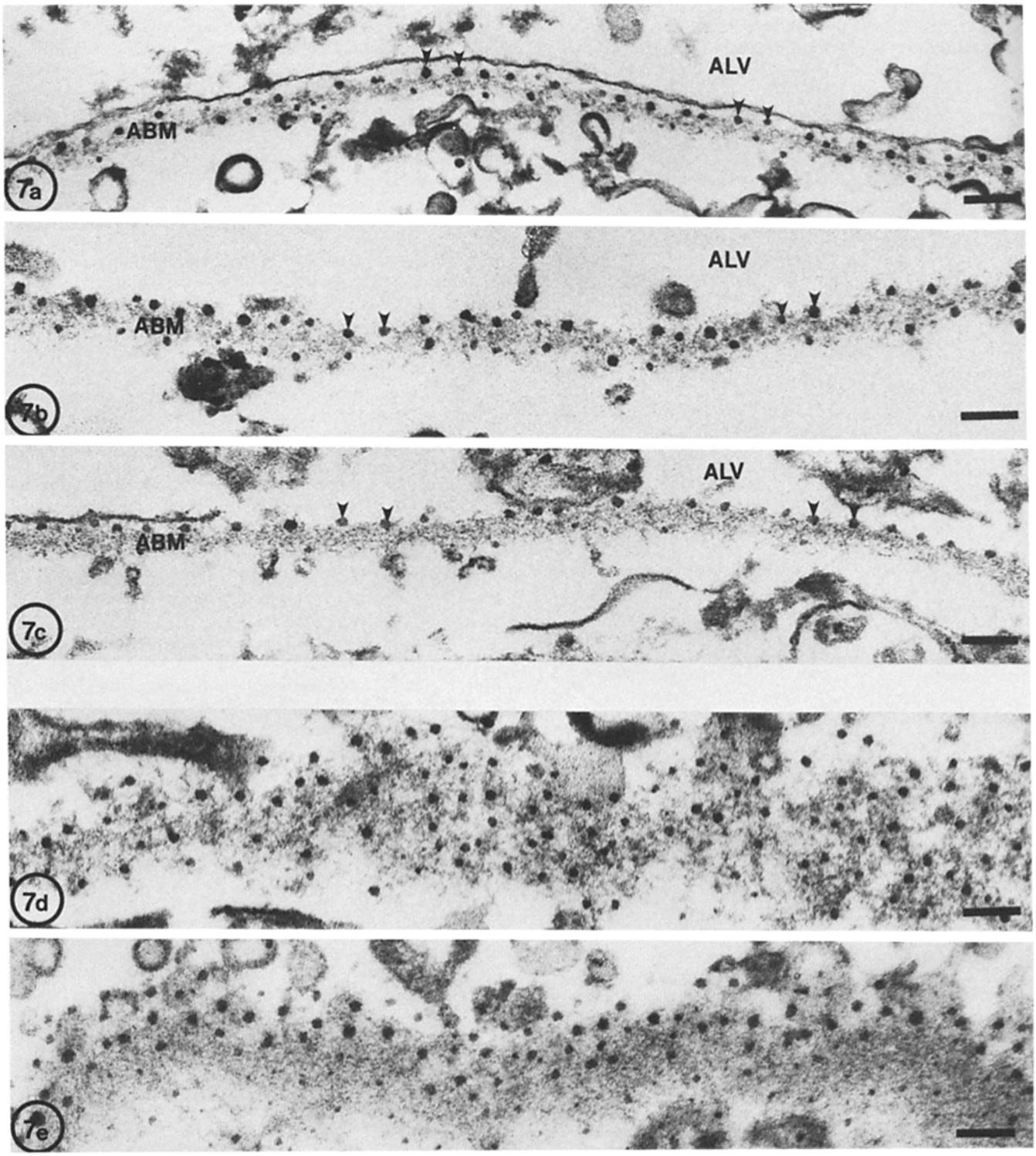

FIGURE 7 Ruthenium red stains of *ABM* at different ages. (*a*) Birth, (*b*) 8 d, (*c*) adult. *ABM* has ordered array of ruthenium red-positive granules (arrow heads) representing anionic sites lie in the lamina rara and at birth are distributed evenly on epithelial or luminal and interstitial or abluminal side of the lamina densa. The alveolus (*ALV*) is noted in each section. In the adult most ruthenium red positive granules lie in the lamina rara externa on the luminal side of the *ABM*. (*d*) Birth, (*e*) adult. Slant cuts of ABM showing ruthenium red positive granules dispersed evenly at birth but localized on the luminal side of the ABM in the adult. Bars, 0.1 μm. × 103,420.

Thereafter, further growth of the lung is associated with enlargement of alveoli and lengthening of capillaries within their CBM sheath, but new vessels and new alveoli no longer form. Thus the completed CBM may serve as a barrier to new vessel formation and prevent formation of new alveoli in the adult.

ABM Proteoglycans

A third major morphologic change in the ABM relates to the decrease in abluminal heparan sulfate proteoglycans that occurs with age. There is a 47% decrease in abluminal ABM

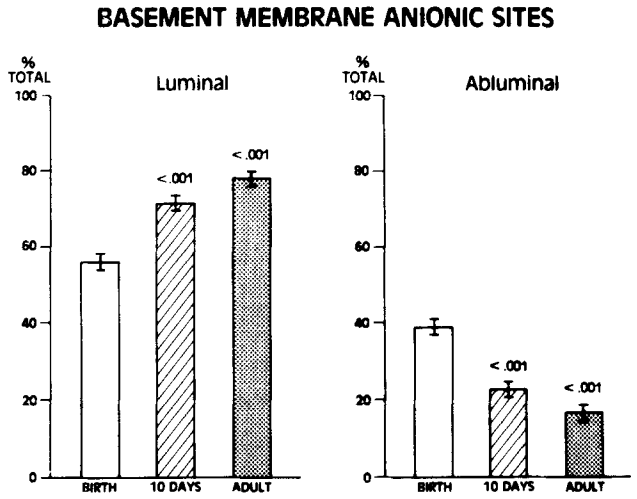

FIGURE 8 Distribution of ruthenium red-positive anionic sites on luminal and abluminal side of ABM lamina densa at birth, 10 d, and in adult. Mean values ± 1 SEM. Values at two older ages are significantly different from those at birth ($p < .001$).

TABLE I

Morphometric Analysis of ABM Anionic Sites

	No. of sites/nm	
	Luminal	Abluminal
Birth (28)		
$\bar{x}$	1.43	1.01
SEM	0.04	0.03
8 d (29)		
$\bar{x}$	1.61*	0.53*
SEM	0.04	0.04
Adult (30)		
$\bar{x}$	1.68*	0.38*‡
SEM	0.04	0.03

Linear density of ruthenium red-positive sites on the luminal (lamina rara externa) and abluminal (lamina rara internal) side of the ABM. Numbers in parentheses represent segments of ABM analyzed at each age. Values represent mean ($\bar{x}$) and 2 SEM.

* $p < .001$ vs. birth.

‡ $p < .001$ vs. 8 d.

anionic site density between birth and 8 d of age and 73% decrease between birth and the adult. The decrease occurs in ABM beneath both types-1 and -2 cells, again supporting their common origin. This selective decrease in abluminal sites without change in luminal sites could represent either a loss of preexisting abluminal proteoglycans, perhaps because little interstitial collagen is present to stabilize these sites (44), or diminished production of abluminal heparan sulfate proteoglycans as new ABM is synthesized during the 10-fold increase in alveolar surface area between birth and 6 wk of age (2).

The abluminal heparan sulfate proteoglycans could serve a variety of functions but the timing of change in these proteoglycans suggests that they may be involved in postnatal structuring of the alveolar gas exchange surface. One such function might relate to cell-substrate adhesion regulating the formation of the "thin side" of the alveolar wall where endothelial cells lie immediately adjacent to alveolar epithelium separated only by the ABM, because glycosaminoglycans have been shown to influence cell adhesion (45–47). A second function of abluminal heparan sulfate proteoglycans may also relate to formation of the thin gas exchange side of the alveolar wall.

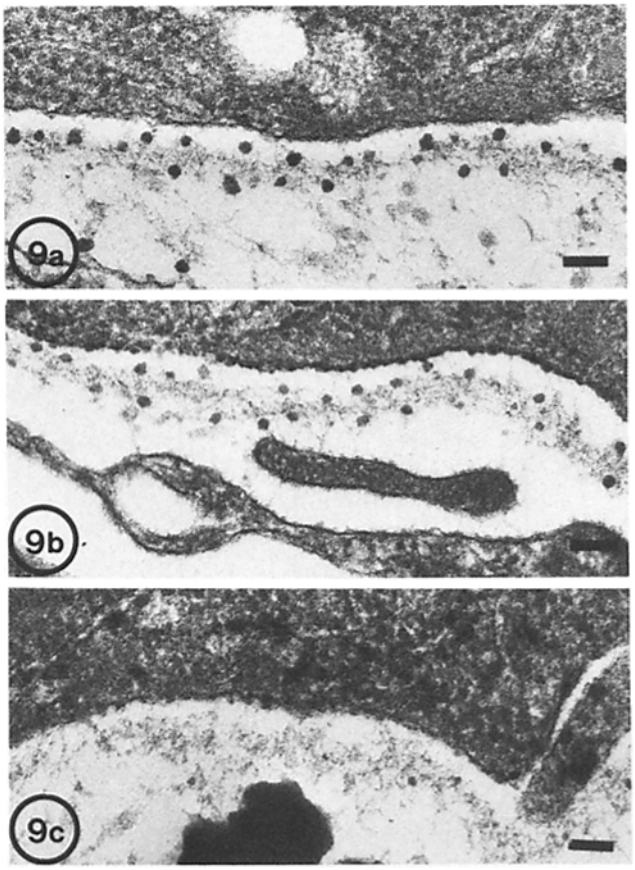

FIGURE 9 ABM from newborn rat lung subject to selective enzyme degradation prior to staining with ruthenium red. Compared with control samples (*a*), anionic sites associated with the ABM resist digestion with chondroitinase ABC (*b*). Incubation with F. heparium enzyme removes all ABM associated anionic sites (*c*). Bars, 0.1 μm. × 59,690.

TABLE II

Formation of [^{35}S]Proteoglycans

	ng Protein	mg DNA per mg protein	cpm × 10^{-3} per mg protein	cpm × 10^{-3} per mg DNA	Heparan sulfate as % of total [^{35}S]proteoglycans
Newborn	0.9	55	570	10.4	27
8 D	0.9	45	200	5.7	31
Adult	3.1	19	39	2.1	26

Capillary endothelium is gradually encompassed by CBM during the postnatal period except when it is in close approximation to the ABM. There, no CBM appears and the gas exchange surface that is formed consists of epithelium, a single ABM, and endothelium. It is possible that CBM is made, but does not stabilize adjacent to ABM because of the high density of abluminal heparan sulfate proteoglycans. Several studies have shown that glycosaminoglycans may play an important role in regulating collagen formation (48–50) although no information exists about their effect of type-IV collagen assembly.

Our studies suggest that basement membranes of the alveolar wall are intimately involved in the postnatal structuring of the

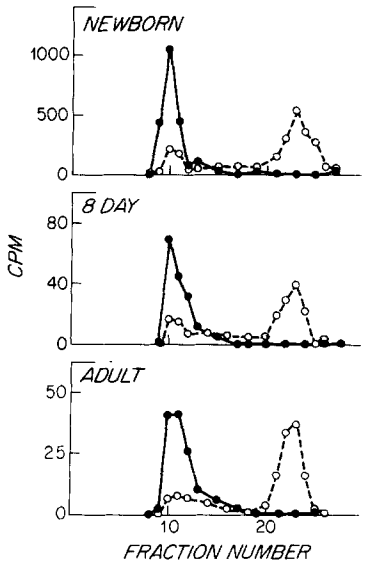

FIGURE 10 Radioactivity in effluent of Sephadex G-50 column from [^{35}S]glycosaminoglycans incubated with PBS (●) or with chondroitinase ABC (○) at three different ages. Glycosaminoglycans remaining in the area of fraction ten following incubation with chondroitinase represent heparan sulfate. All labeled glycosaminoglycans were degraded following incubation with *F. heparium* enzyme. The percent of [^{35}S]glycosaminoglycans not degraded by chondroitinase ABC is similar at all ages.

lung associated with formation of its gas exchange surfaces. It is likely that epithelial-mesenchymal interactions established through the ABM are involved with cytodifferentiation of the alveolar epithelium and may also be involved in the production of the ABM itself. Changes in CBM suggest that angiogenesis is a major facet of early postnatal lung growth and perhaps a controller of alveolar formation. It is likely that ABM-associated heparan sulfate proteoglycans, and perhaps other ABM glycoproteins not visualized in these studies, are involved in structuring of the thin gas exchange surface of the lung as new alveoli form. The links between alveolar formation and basement membrane modification also suggest that the changes we have described may be associated with the inability of the mature lung to form new alveoli.

This work was supported by National Heart Lung and Blood Institute grants HL 19717 and HL 07035.

Received for publication 12 April 1982, and in revised form 7 July 1982.

REFERENCES

1. Thurlbeck, W. M. 1975. Postnatal growth and development of the lung. *Am. Rev. Respir. Dis.* 111:803–844.
2. Burri, P. H., J. Dhaly, and E. R. Weibel. 1974. The postnatal growth of the rat lung. I. Morphometry. *Anat. Rec.* 178:711–730.
3. Buhain, W. J., and J. S. Brody. 1973. Compensatory growth of the lung following pneumonectomy. *J. Appl. Physiol.* 35:898–902.
4. Hay, E. D. 1978. Role of basement membranes in development and differentiation. *In* Biology and Chemistry of Basement Membranes. N. A. Kefalides, editor. Academic Press, New York. 119–136.
5. Hay, E. D., and S. Meier. 1976. Stimulation of corneal differentiation by interaction between cell surface and extracellular matrix. *Dev. Biol.* 52:141–157.
6. Thesleff, I., H. J. Barrach, J. M. Foidart, A. Vaheri, P. M. Pratt, and G. R. Martin. 1981. Changes in the distribution of Type IV collagen, laminin, proteoglycan, and fibronectin during mouse tooth development. *Dev. Biol.* 81:182–192.
7. Ekbloom, P. 1981. Formation of basement membranes in the embryonic kidney: an immunohistological study. *J. Cell Biol.* 91:1–10.
8. Saxen, L., and E. Lehtoren. 1978. Transfilter induction of kidney tubules as a function of the extent and duration of intercellular contacts. *J. Embryol. Exp. Morphol.* 47:97–109.
9. Banerjee, S. D., R. H. Cohen, and M. R. Bernfield. 1977. Basal lamina of embryonic salivary epithelia: production by the epithelium and role in maintaining lobular morphology. *J. Cell Biol.* 73:445–463.
10. Bernfield, M. R., and S. D. Banerjee. 1978. The basal lamina in epithelial-mesenchymal morphogenic interactions. *In* Biology and Chemistry of Basement Membranes. N. S. Kefalides, editor. Academic Press, New York. 137–148.
11. Wicha, M. S., L. A. Liotta, B. K. Vonderhaar, and W. R. Kidwell. 1980. Effects of inhibition of basement membrane collagen deposition on rat mammary gland development. *Dev. Biol.* 80:253–266.
12. Alescio, T., and A. Cassini. 1962. Induction in vitro of tracheal buds by pulmonary mesenchyme grafted on tracheal epithelium. *J. Exp. Zool.* 150:83–94.
13. Bluemink, J. G., P. V. Maurik, and K. A. Lawson. 1976. Intimate cell contacts at the epithelial/mesenchymal interface in embryonic mouse lung. *J. Ultrastruct. Res.* 55:257–270.
14. Masters, J. R. W. 1976. Epithelial-mesenchymal interaction during lung development: the effect of mesenchymal mass. *Dev. Biol.* 51:48–108.
15. Wessels, N. K. 1970. Mammalian lung development: interaction in formation and morphogenesis of tracheal buds. *J. Exp. Zool.* 175:455–466.
16. Vaccaro, C. A., and J. S. Brody. 1979. Ultrastructural localization and characterization of proteoglycans in the pulmonary alveolus. *Am. Rev. Respir. Dis.* 120:901–910.
17. Vaccaro, C. A., and J. S. Brody. 1981. Structural features of alveolar wall basement membrane in the adult rat. *J. Cell Biol.* 91:427–437.
18. Burri, P. J. 1974. The postnatal growth of the rat lung. III. Morphology. *Anat. Rec.* 180:77–98.
19. Nardell, E. A., and J. S. Brody. 1982. Determinants of the mechanical properties of the rat lung during postnatal development. *J. Appl. Physiol.* In press.
20. Suzuki, S. 1972. Chondroitinases from proteus vulgaris and *Flavobacterium heparinum*. *Methods Enzymol.* 28:911–917.
21. Gill, P. J., J. Adler, C. K. Silbert, and J. E. Silbert. 1981. Removal of glycosaminoglycans from cultures of human skin fibroblasts. *Biochem. J.* 194:299–307.
22. Linker, A., and P. Hovingh. 1972. Heparinase and heparitinase from Flavobacteria. *Methods Enzymol.* 28:903–911.
23. Sugrue, S. P., and E. D. Hay. 1981. Response of basal epithelial cell surface and cytoskeleton to solubilized extracellular matrix molecules. *J. Cell Biol.* 91:45–54.
24. Merrilees, M. J., and L. Scott. 1980. Interaction of epithelial cells and fibroblasts in culture: effect on glycosaminoglycan levels. *Dev. Biol.* 76:396–409.
25. Johnson-Muller, B., and J. Gross. 1978. Regulation of corneal collagenase production: epithelial-stromal cell interaction. *Proc. Natl. Acad. Sci. U. S. A.* 75:4417–4421.
26. Solursen, M., C. T. Singley, and R. S. Reiter. 1981. The influence of epithelia on cartilage and loose connective tissue formation by limb mesenchyme cultures. *Dev. Biol.* 86:471–482.
27. Alquier, C., G. Fayet, S. Horsepian, and M. Michel-Bechet. 1979. Biosynthesis of the basal lamina as a result of interaction between thyroid and mesenchymal cells in culture. *Cell Tissue Res.* 200:69–81.
28. Cutler, L. S. 1980. The dependent and independent relationships between cytodifferentiation and morphogenesis in developing salivary gland secretory cells. *Anat. Rec.* 196:341–347.
29. Smith, B. T. 1979. Lung maturation in the fetal rat: acceleration by injection of fibroblast-pneumonectomy factor. *Science (Wash. D. C.).* 204:1094–1095.
30. Smith, B. T., W. Galaugher, and W. M. Thurlbeck. 1980. Serum from pneumonectomized rabbits stimulates alveolar type II cell proliferation in vitro. *Am. Rev. Respir. Dis.* 121:701–707.
31. Mason, R. J., and M. C. Williams. 1977. Type II alveolar cell. Defender of the alveolus. *Am. Rev. Respir. Dis.* 115:77–91.
32. Adamson, I. Y. R., and D. H. Bowden. 1975. Derivation of type 1 epithelium from type 2 cells in the developing rat lung. *Lab. Invest.* 32:736–745.
33. Kauffman, S. L., P. H. Burri, and E. R. Weibel. 1974. The postnatal growth of the rat lung. II. Autoradiograph. *Anat. Rec.* 1808:63–76.
34. Brody, J. S., R. Burki, and N. Kaplan. 1978. Deoxyribonucleic acid synthesis in lung cells during compensatory lung growth after pneumonectomy. *Am. Rev. Respir. Dis.* 117:307–316.
35. Adamson, I. Y. R., and D. H. Bowden. 1974. The type 2 cell as a progenitor of alveolar epithelial regeneration: A cytodynamic study in mice after exposure to oxygen. *Lab. Invest.* 30:35–42.
36. Evans, M. J., L. J. Cabral, R. J. Stephens, and G. Freeman. 1975. Transformation of alveolar type 2 cells to type 1 cells following exposure to NO_2. *Exp. Mol. Pathol.* 22:142–150.
37. Haies, D. M., J. Gil, and E. R. Weibel. 1981. Morphometric study of rat lung cells: I. Numerical and dimensional characteristics of parenchymal cell population. *Am. Rev. Respir. Dis.* 123:533–541.
38. Williams, M. C., and R. J. Mason. 1977. Development of the type II cell in the fetal rat lung. *Am. Rev. Respir. Dis.* 115 (part 2):37–47.
39. Strang, L. B. 1977. Growth and development of the lung: fetal and postnatal. *Annu. Rev. Physiol.* 39:253–276.
40. Grant, M. M., N. Roth, and J. S. Brody. 1981. Basement membrane development in fetal rat lungs. *Fed. Proc.* 40:468.
41. Farin, F. M., G. E. Striker, A. B. Fisher, and H. Sage. 1981. Biosynthesis of extracellular matrix components by granular pneumonocytes in vitro. *Fed. Proc.* 40:767.
42. Ausprunk, D. H., G. I. Boudreau, and D. A. Nelson. 1981. Proteoglycans in the microvasculature. II. Histochemical localization in proliferating capillaries of the rabbit cornea. *Am. J. Pathol.* 103:367–375.
43. Ausprunk, D. H., and J. Folkman. 1977. Migration and proliferation of endothelial cells in preformed and newly formed blood vessels during tumor angiogenesis. *Microvasc. Res.* 14:53–65.
44. David, G., and M. R. Bernfield. 1979. Collagen reduces glycosaminoglycan degradation by cultured mammary epithelial cells: possible mechanism for basal lamina formation. *Proc. Natl. Acad. Sci. U. S. A.* 76:786–790.
45. Kleinman, H. K., R. J. Klebe, and G. R. Martin. 1981. Role of collagenous matrices in the adhesion and growth of cells. *J. Cell Biol.* 88:473–485.
46. Culp, L. A., B. J. Rollins, J. Buriel, and S. Hitri. 1978. Two functionally distinct pools of glycosaminoglycans in the substrate adhesion site of murine cells. *J. Cell Biol.* 79:788–801.
47. Schubert, D., and M. La Corbiere. 1980. A role of secreted glycosaminoglycans in cell-substratum adhesion. *J. Biol. Chem.* 255:11564–11569.
48. Handley, C. J., P. Brooks, and D. A. Lowther. 1980. Suppression of collagen synthesis by chondrocytes by exogenous concentrations of proteoglycan subunit. *Biochem. Int.* 1:270–276.
49. Lilja, S., and H. J. Barrach. 1981. An electron microscopical study of the influence of different glycosaminoglycans on the fibrillogenesis of collagen type I and II in vitro. *Virchows Arch. Pathol. Anat.* 390:325–338.
50. Oegema, T. R., J. Laidlaw, V. C. Hascall, and D. D. Dziewiatkowski. 1975. The effect of proteoglycans on the formation of fibrils from collagen solutions. *Arch. Biochem. Biophys.* 170:698–709.